DOCUMENT CONTROL DATA - R & D

(Security classification of title, body of abstract and indexing annotation must be entered when the overall report is classified)

1

1. ORIGINATING ACTIVITY (Corporate author)	2a. REPORT SECURITY CLASSIFICATION
Aerospace Medical Research Laboratory Aerospace Medical Div, Air Force Systems Command Wright-Patterson Air Force Base, Ohio 45433	Unclassified 2b. GROUP N/A

AD 744461

3. REPORT TITLE

THE TRANSVERSE RESPONSE OF THE LUMBAR SPINE UNDER LONGITUDINAL LOADS.

4. DESCRIPTIVE NOTES (Type of report and inclusive dates)

5. AUTHOR(S) (First name, middle initial, last name)

H. E. Krause
M. Shirazi

6. REPORT DATE	7a. TOTAL NO. OF PAGES	7b. NO. OF REFS
December 1971	~~27~~ 31	6

8a. CONTRACT OR GRANT NO.	9a. ORIGINATOR'S REPORT NUMBER(S)
b. PROJECT NO. 7231	AMRL-TR-71-29 Paper No. 24
c.	9b. OTHER REPORT NO(S) (Any other numbers that may be assigned this report)
d.	

10. DISTRIBUTION STATEMENT

Approved for public release; distribution unlimited

11. SUPPLEMENTARY NOTES	12. SPONSORING MILITARY ACTIVITY
	Aerospace Medical Research Laboratory Aerospace Medical Div, Air Force Systems Command, Wright-Patterson AFB, OH 45433

13. ABSTRACT

The Symposium on Biodynamics Models and Their Applications took place in Dayton, Ohio, on 26-28 October 1970 under the sponsorship of the National Academy of Sciences - National Research Council, Committee on Hearing, Bioacoustics, and Biomechanics; the National Aeronautics and Space Administration; and the Aerospace Medical Research Laboratory, Aerospace Medical Division, United States Air Force. Most technical areas discussed included application of biodynamic models for the establishment of environmental exposure limits, models for interpretation of animal, dummy, and operational experiments, mechanical characterization of living tissue and isolated organs, models to describe man's response to impact, blast, and acoustic energy, and performance in biodynamic environments.

31

DD FORM 1 NOV 68 1473

Security Classification

3

PAPER NO. 24

THE TRANSVERSE RESPONSE OF THE LUMBAR SPINE UNDER LONGITUDINAL LOADS

H. E. Krause and M. Shirazi

University of Dayton Research Institute
Dayton, Ohio

ABSTRACT

A novel continuous model of the spine is presented. The transverse motion in the sagittal plane of the spine of sitting human subjects exposed to vertical vibrations revealed considerable bending along the lumbar spine and negligible bending along the thoracic spine. Therefore, the model consists of a curved rod, representing the lumbar spine, longitudinally loaded by a mass, representing the thorax. The differential equation of the transverse motion was derived and solved by making a product assumption. No transverse displacements and no bending moment was assumed at the pelvic end. At the thoracic end, a shear force and a bending moment are applied, representing translatory and rotatory inertia of the attached rib cage.

Eigenfunctions and eigenvalues depend on longitudinal loading. The eigenfunctions correlate well with data obtained over a large range of experimental conditions. The solution for the time distribution contains various distinct harmonic components if an external force, alternating sinusoidally at only one discrete frequency, is applied. This effect is due to a periodic parameter in the differential equation.

INTRODUCTION

Most observed spinal injuries result from external forces applied in the longitudinal direction. Long-time exposure to moderate external loads can develop slowly increasing damages. Compression of the spinal column is the prevailing stress mode.

In recent tests, Vulcan et al.[1] observed considerable bending of the spine of human cadavers that were exposed to spinal-direction impact. Considerable bending of the lumbar spine of sitting human subjects under vertical vibrations was observed by Krause.[2] In view of these findings it seems that transverse displacements as well as longitudinal displacements should be considered.

Bending relieves stress in certain areas and increases it in others, if it is superimposed on existing compression. Therefore, bending may be the factor that determines the location of injury if it is present to a significant magnitude.

This is an exploratory study in which only transverse responses under longitudinal loads will be considered. In particular, we attempt to account quantitatively for the effect of a longitudinal load and initial curvature on the bending stress, its distribution along the lumbar spine, and the conditions of dynamic instability. Longitudinal responses will be neglected. It has been shown by Bolotin[3] that transverse vibrations are significantly disturbed by longitudinal vibrations only at resonance of the latter. Longitudinal vibrations can therefore be neglected if we assume their resonant frequencies and those of the transverse vibrations do not coincide.

SPINAL MODEL CONFIGURATION

For a hypothesis, a spine model is assumed that consists of two parts (Figure 1). They are a curved rod to represent the lumbar spine, and a rigid mass connected with it that represents the thorax.

Experimental observations have led to this configuration (Figure 2). The amplitude of the first derivative of the transverse displacement of the thoracic spine above the 10th thoracic vertebra of a sitting human subject under vertical vibrations from 10 to 40 Hz is almost constant. The second derivative is, therefore, almost zero and hardly any bending exists. It is assumed that the rib cage increases the bending stiffness of that part of the spinal column.

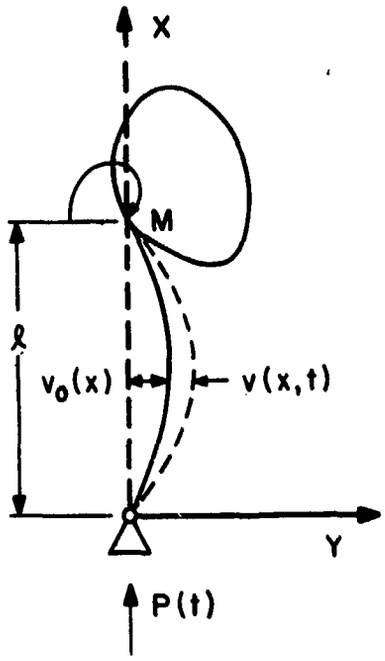

Figure 1. Model Configuration for Lumbar Spine and Thorax.

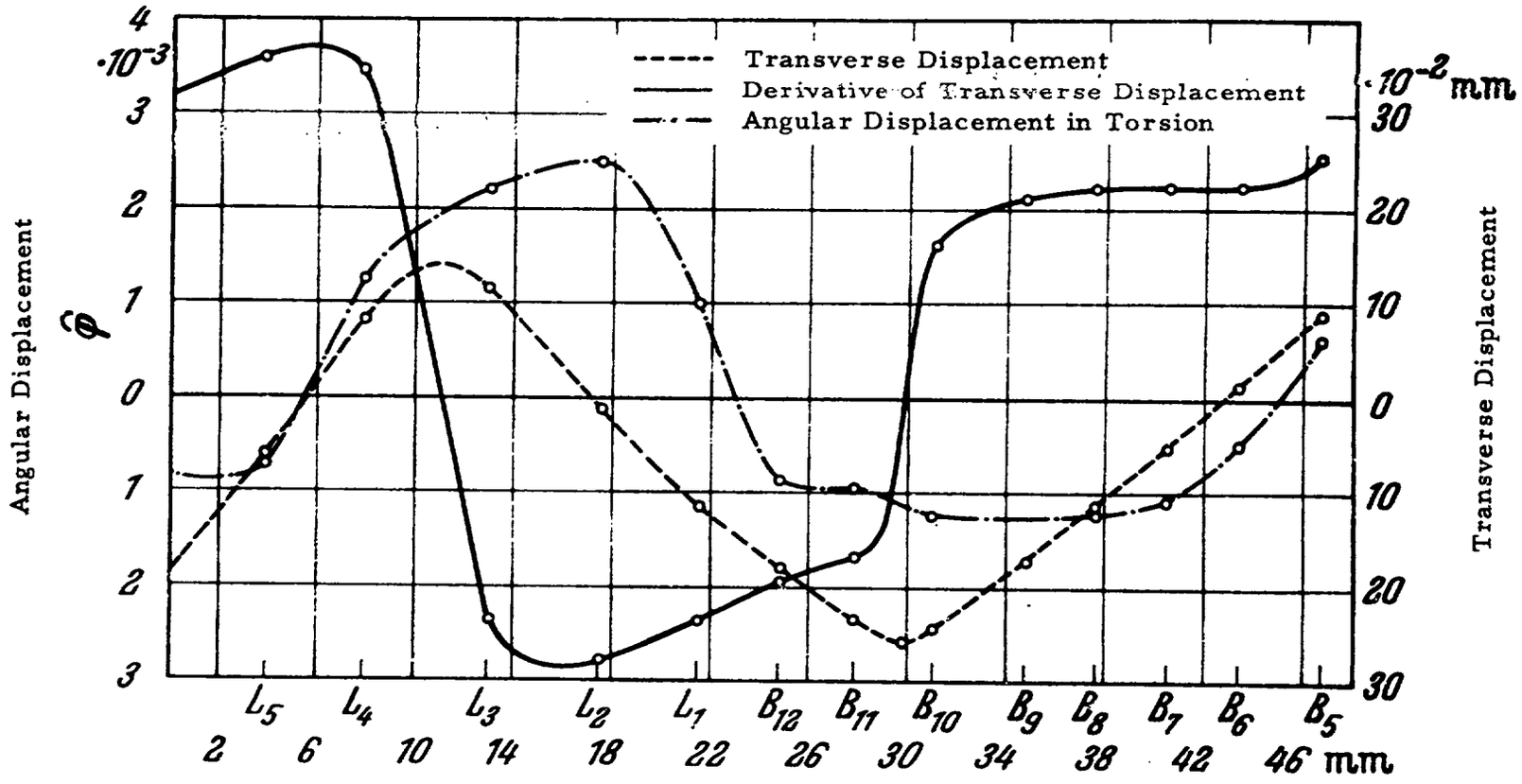

Figure 2. Transverse and Torsional Vibration Amplitude Along the Spine. Ref. 2

It should be noted that Figure 2 includes the torsional deflection under the same experimental conditions. A nodal point can be observed around the 6th and 5th thoracic vertebra. This point was observed for 13 frequencies within the test range from 10 and 40 Hz and for 30 experiments at each frequency. This nodal point coincides with a peak at that point of almost all published curves of injury incidence along the spinal column.

EQUATION OF MOTION

The equation of transverse motion of a curved beam has been presented by Bolotin.[3] It is

$$EI \frac{\partial^4 v}{\partial x^4} + P(t) \frac{\partial^2 v}{\partial x^2} + \mu \frac{\partial^2 v}{\partial t^2} = - P(t) \frac{d^2 v_o}{dx^2} \qquad (1)$$

where

E = modulus of elasticity

I = aereal moment of inertia

$v(x, t)$ = transverse displacement from initial curvature

$v_o(x)$ = initial curvature

$P(t)$ = longitudinal load (compression positive)

μ = mass per unit length of rod.

The function $v_o(x) = 0$ if the beam is straight. The nonhomogeneous equation (1) reduces to a homogeneous equation

$$EI \frac{\partial^4 v}{\partial x^4} + P(t) \frac{\partial^2 v}{\partial x^2} + \mu \frac{\partial^2 v}{\partial t^2} = 0 . \qquad (2)$$

A product assumption

$$v(x,t) = \sum_{n=1}^{\infty} V_n(x) T_n(t) \qquad (3)$$

where

$V_n(x)$ = spatial distribution

$T_n(t)$ = time distribution,

decomposes the partial differential equation into a system of ordinary ones. They are

$$\frac{EI}{\mu} V_n^{(4)}(x) + \frac{P(t)}{\mu} V_n'' - \Omega_n^2 V_n = 0 \tag{4}$$

$$\ddot{T}_n + \Omega_n^2 T_n = 0 \tag{5}$$

P(t) is here considered to be constant.

The solutions for these equations are

A. Spatial Distribution

$$V_n(x) = D_{1n} \sin r_2 x + D_{2n} \cos r_2 x \tag{6}$$

$$+ D_{3n} \sinh r_1 x + D_{4n} \cosh r_1 x$$

The r_1 and r_2 are

$$r_{1,2} = \sqrt{-\frac{P}{2EI} + \sqrt{\left(\frac{P}{2EI}\right)^2 + \frac{\mu\Omega^2}{EI}}} \tag{7}$$

B. Time Distribution

$$T_n(t) = A_{1n} \cos \Omega_n t + A_{2n} \sin \Omega_n t \tag{8}$$

where

Ω_n = natural frequencies

D_{mn} = constants

r_1, r_2 = eigenvalues

The constants D_{mn} will have to be determined by the boundary conditions. Two different sets of boundary conditions will be considered in the following sections. A solution for the homogeneous (that is, straight beam) equation of motion and for the nonhomogeneous (that is, curved beam) equation of motion will be derived for each set of boundary conditions.

RESTRAINED THORAX

The thorax is supposed to be restrained so that no transverse displacement or rotation can occur. The idealized model for the lumbar spine under these conditions is depicted in Figure 3. This configuration has been treated extensively by Bolotin[3] and other researchers in the field of dynamic instability with the inclusion of nonlinear damping and nonlinear inertia.

A. Straight Rod

The solutions for the constants in the spatial distribution equation for the straight beam (equation 6) are determined by the boundary conditions which are

$$V(\ell) = V(0) = 0$$

$$\left(\frac{d^2V}{dx^2}\right)_{x=\ell} = \left(\frac{d^2V}{dx^2}\right)_{x=0} = 0 . \tag{9}$$

Transverse displacements and bending moments are not admitted at either end of the lumbar spine. This furnishes the equations:

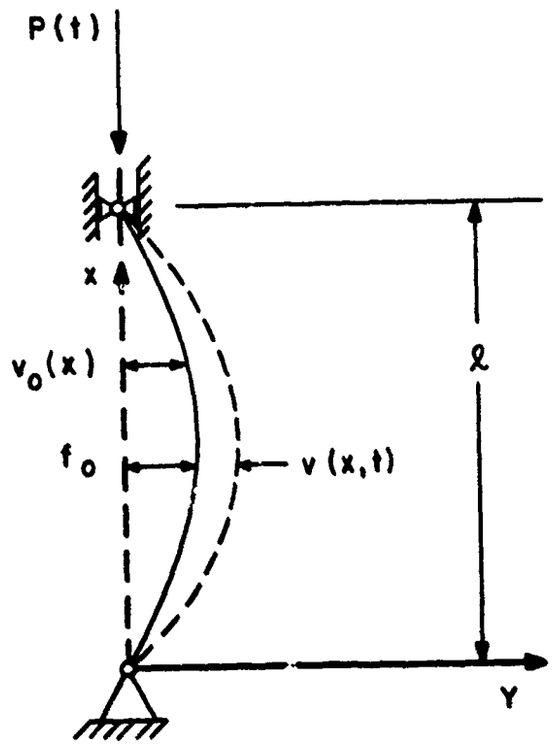

Figure 3. Model Configuration of Lumbar Spine, with Thorax Restrained from Moving.

$$V(\ell) = 0 = D_1 \sin r_2 \ell + D_2 \cos r_2 \ell + D_3 \sin h\, r_1 \ell + D_4 \cos h\, r_1 \ell \tag{10}$$

$$V(0) = 0 = D_2 + D_4 \tag{11}$$

$$V''(\ell) = 0 = -D_1 r_2^2 \sin r_2 \ell - D_2 r_2^2 \cos r_2 \ell + D_3 r_1^2 \sin h\, r_1 \ell + D_4 r_1^2 \cos h\, r_1 \ell \tag{12}$$

$$V''(0) = 0 = -D_2 r_2^2 + D_4 r_1^2 \,. \tag{13}$$

These are four homogeneous equations for the four unknowns. In order to obtain solutions, the characteristic determinant has to be zero.

$$\Delta = 0 = \begin{vmatrix} 0 & 1 & 0 & 1 \\ 0 & -r_2^2 & 0 & r_1^2 \\ \sin r_2 \ell & \cos r_2 \ell & \sin h r_1 \ell & \cos h r_1 \ell \\ -r_2^2 \sin r_2 \ell & -r_2^2 \cos r_2 \ell & +r_1^2 \sin h r_1 \ell & r_1^2 \cos h r_1 \ell \end{vmatrix}$$

$$\Delta = +(r_1^2 + r_2^2)^2 \sin r_2 \ell \sin h r_1 \ell = 0 \tag{14}$$

This condition is met if

$$r_2 \ell = n\pi \tag{15}$$

or

$$r_1 \ell = 0 \tag{16}$$

The latter condition requires P = 0 and is, therefore, trivial. The eigenvalues are:

$$r_2 = \frac{n\pi}{\ell} = \sqrt{\frac{P}{2EI} + \sqrt{\left(\frac{P}{2EI}\right)^2 + \frac{\mu\Omega^2}{EI}}} \tag{17}$$

This equation can be solved for the natural frequencies

$$\Omega_n^2 = \frac{(2EI\,(\frac{n\pi}{\ell})^2 - P)^2 - P^2}{4EI\mu} \quad . \tag{18}$$

It is apparent that these frequencies depend on P. If P is zero, we obtain

$$\Omega_{n0}^2 = (n\frac{\pi}{\ell})^4 \frac{EI}{\mu} \quad . \tag{19}$$

The frequency equation can be rearranged to assume the following form:

$$\Omega_n^2 = (\frac{n\pi}{\ell})^4 \frac{EI}{\mu} - (\frac{n\pi}{\ell})^2 \frac{P}{\mu} \quad . \tag{20}$$

The natural frequencies equal those of the straight beam except for

$$(\frac{n\pi}{\ell})^2 \frac{P}{\mu} \, .$$

The relationship between Ω_n and P is parabolic. The solution v(x, t) is of a periodic nature if Ω is real and it is of a non-periodic nature if Ω is imaginary. The transition between both regimes occurs when $\Omega = 0$. This is the case if

$$P = P_{crit} = n^2(\frac{\pi}{\ell})^2 EI \, . \tag{21}$$

For $P > P_{crit}$ we have buckling and for $P < P_{crit}$ the beam is stable. P_{crit} is equal to the Euler buckling load for this type of beam support.

The dependence of the natural frequencies on the longitudinal load may be of practical consequence. For example, the response of the spine to external forces seems to be different under different sustained vertical loads as they occur in a dive, pullout, or tight curve. The amplitude of free vibrations is expected to change with the natural frequency if energy is conserved during transition from one longitudinal load to another.

The eigenfunctions for this model are

$$V_n(x) = \sin r_{2n} x \,. \tag{22}$$

They are identical with the eigenfunctions of the unloaded straight beam. It is easy to see that these functions are orthogonal.

B. Curved Rod

The initial curvature will be considered in the following paragraph by solving the nonhomogeneous equation of motion, equation (1). The boundary conditions remain the same.

Again, a product assumption is made:

$$v(x,t) = \sum_{n=1}^{\infty} V_n(x)\, T_n(t) \,. \tag{23}$$

$V_n(x)$ represents the eigenfunctions that are now known from the preceding paragraph. $T_n(t)$ are solutions that we seek. Considering the orthogonality of the eigenfunctions, this assumption leads to

$$\ddot{T}_n + T_n\left[\left(\frac{n\pi}{\ell}\right)^4 \frac{EI}{\mu} - \left(\frac{n\pi}{\ell}\right)^2 \frac{P}{\mu}\right] = - \frac{\int_0^{\ell} P \frac{d^2 v_0}{dx^2} V_n(x)\, dx}{\mu \int_0^{\ell} V_n^2(x)\, dx} \,. \tag{24}$$

The initial curvature may be represented by a Fourier sine series. This series contains only sine functions because the initial curvature can be an odd function with

$$V_o(0) = V_o(\ell) = 0.$$

The second derivative of the initial curvature is

$$\frac{d^2 v_o(x)}{dx^2} = -\sum_{n=1}^{\infty} g_{on} \sin \frac{n\pi}{\ell} x \quad , \tag{25}$$

which results in a set of differential equations

$$\ddot{T}_n + T_n \left[\left(\frac{n\pi}{\ell}\right)^4 \frac{EI}{\mu} - \left(\frac{n\pi}{\ell}\right)^2 \frac{P(t)}{\mu} \right] = \frac{P(t) g_{on}}{\mu} \quad . \tag{26}$$

These equations are uncoupled due to the orthogonality of the eigenfunctions and due to the orthogonality between the eigenfunctions and the Fourier components of the initial curvature. With the initial conditions

$$v(x,0) = f_1(x) \; ; \quad \left(\frac{\partial v}{\partial t}\right)_{t=0} = f_2(x) \; , \tag{27}$$

we obtain the solution

$$T_n(t) = \frac{2}{\Omega_n \ell} \left(\int_0^{\ell} f_2(x) \sin \frac{n\pi}{\ell} x \, dx \right) \sin \Omega_n t$$

$$+ \left[\frac{2}{\ell} \int_0^{\ell} f_1(x) \sin \frac{n\pi}{\ell} x \, dx - \frac{P g_{on}}{\mu \Omega_n^2} \right] \cos \Omega_n t +$$

$$\frac{P g_{on}}{\mu \Omega_n^2} \quad . \tag{28}$$

The longitudinal load P, as well as the modulus of the Fourier components, is contained in the coefficient of $\cos \Omega_n t$. Thus both of them have an effect on the amplitude of the free motion.

The coefficient of the cosine function of the n^{th} eigenmode contains only the Fourier coefficient of the n^{th} component of the initial curvature. If some of these components are zero, then the equivalent eigenmode amplitude will be unaffected by either the initial curvature or the longitudinal load.

The spine can assume various equilibrium positions. Each one will produce a different shape of its initial curvature. This results in different sets of g_{on} values. The amplitudes of the various eigenmodes and locations of maximum bending stress will therefore be dependent on the attitude of the subject.

In particular, the interpretation of test results with animal subjects should take differences in curvature between man and animal into consideration.

C. Dynamic Instability

When a time variable force is added to the longitudinal load, then

$$P(t) = P + P_0 \sin \omega t \quad . \tag{29}$$

The solution that was just discussed does not apply. The differential equation for the time distribution is now

$$\ddot{T} + T\left[\left(\frac{n\pi}{l}\right)^4 \frac{EI}{\mu} - \left(\frac{n\pi}{l}\right)^2 (P + P_0 \sin \omega t)\frac{1}{\mu}\right] =$$

$$(P + P_0 \sin \omega t)\frac{f_0 \pi^2}{\mu l^2} \quad . \tag{30}$$

This equation represents a Mathieu equation except for the addition of a forcing function. Due to the multiplicative connection of T and its coefficient, the solution contains also harmonics that are of different frequency than the parameter variation. Which one of these harmonics dominates the solution depends on the relation of the parameter frequency to the natural frequency. Unbounded solutions can be expected at and around frequencies that, according to Bolotin[3], are

$$\omega = \frac{2\Omega}{k} \qquad , k = 1, 2, 3 \ldots \tag{31}$$

The solution is of frequency ω if k is even and of frequency $\omega/2$ if k is odd. Therefore there are frequencies of parametric resonance in addition to the regular resonant frequencies. These frequencies are load-dependent. The relationship between the first resonant frequency and the longitudinal load, equation (20), is represented by the solid parabola (Figure 4) that intersects the abscissa at $\omega/\Omega = 1$. The other parabolas represent locations of possible parametric resonance.

Instability is also possible in areas around these parabolas. Their width depends on the amplitude P_o of the load variation. These regions of instability are indicated by the shaded areas in Figure 4. Most dangerous, is the first region of instability that is represented by the first region on the right.

Approximate equations for the boundaries between the stable and unstable regions are given by Bolotin[3]. They are:

1st Region of Instability:

$$\omega = 2\Omega\sqrt{(1-\frac{P}{P_E})(1\pm\frac{\epsilon}{2})} \tag{32}$$

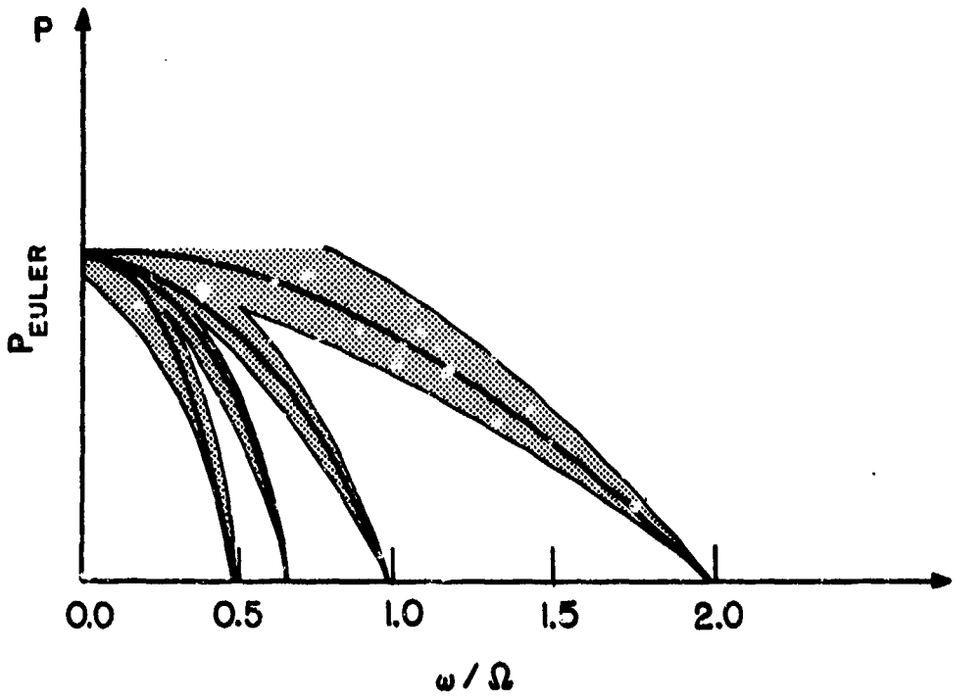

Figure 4. Regions of Instability for Model of Lumbar Spine (Thorax Restrained).

2nd Region of Instability:

$$\omega = \Omega\sqrt{(1-\frac{P}{P_E})(1+\frac{1}{3}\epsilon^2)}$$

$$\omega = \Omega\sqrt{(1-\frac{P}{P_E})(1-2\epsilon^2)} \qquad (33)$$

3rd Region of Instability:

$$\omega = \frac{2}{3}\Omega\sqrt{(1-\frac{P}{P_E})(1-\frac{9\epsilon^2}{8+9\epsilon})} \qquad (34)$$

$$\epsilon = \frac{P_0}{2(P-P_E)} \quad ; \; P_E \text{ Euler buckling Load .}$$

Parametric resonances were occasionally observed when the transverse motion of the spine of a human subject under vertical vibrations was observed. The difference of impedance curves as obtained through vibration and impact tests could perhaps be explained through parametric excitation.

Also the capability of the spine to transfer energy at various frequencies may be of some consequence, in particular with respect to subsystems that are coupled to the spine. Conversely, coupled subsystems may distort parametric resonances.

UNRESTRAINED SPINE

The model will now be extended to include the thorax without external restraints. The boundary conditions at the upper end of the rod are determined by the inertia of the thoracic mass to transverse accelerations and the rotational inertia of the thorax (Figure 1). A longitudinal force is acting at the lower end of the lumbar spine. The configuration is somewhat idealized because whole-body accelerations and rotations are assumed to be negligible. The equation of motion is the same as in the previous case and the treatment will follow the

same sequence of steps as before. The homogeneous equation of motion, equation (2), (straight rod) will be solved first and the effects of the longitudinal loading will be discussed. The second step is the solution of the nonhomogeneous equation of motion, equation (1), and a discussion of the results.

A. Straight Rod

Equation (2) applies in this case as well as the ordinary differential equations (4) and (5) that were derived from it, and the general solution for the spatial distribution, equation (6), and time distribution, equation (7). The constants D_{mn} will have to be determined by the boundary conditions which were discussed in the previous paragraph, and are quantitatively defined by the following equations:

$$V(0) = V''(0) = 0 \tag{35}$$

$$EI\left(\frac{\partial^3 V}{\partial x^3}\right)_{x=l} = -m\left(\frac{\partial^2 V}{\partial t^2}\right)_{x=l} \tag{36}$$

m – mass of thorax

$$\theta\left(\frac{\partial^3 V}{\partial x \partial t^2}\right)_{x=l} = -EI\left(\frac{\partial^2 V}{\partial x^2}\right)_{x=l} \tag{37}$$

θ – dynamic moment of inertia of thorax

The characteristic equation as obtained through the usual manipulation is

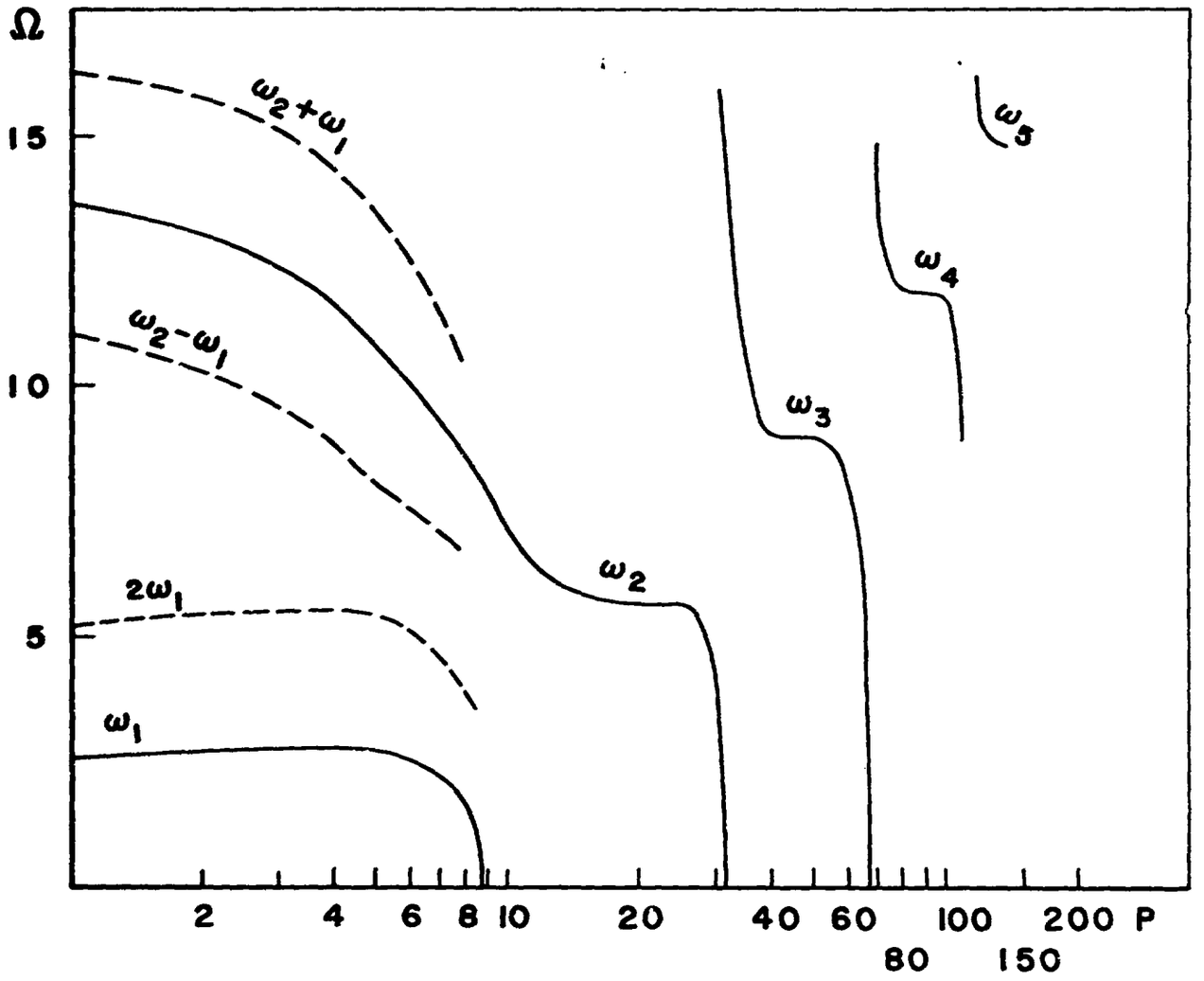

Figure 5. Curves of Possible Instability for the Unrestrained Spine Model.

$$(r_1^2 + r_2^2)\left[(-r_2^3 \cos r_2 \ell - \delta \sin r_2 \ell)(r_1^2 \sinh r_1 \ell - \lambda r_1 \cosh r_1 \ell) + (r_1^3 \cosh r_1 \ell - \delta \sinh r_1 \ell)\cdot(r_2^2 \sin r_2 \ell + \lambda r_2 \cos r_2 \ell)\right] = 0 \qquad (38)$$

In this equation are

$$\delta = \frac{m\Omega_n^2}{EI} \qquad (39)$$

$$\lambda = \frac{\theta\Omega_n^2}{EI} \qquad (40)$$

The characteristic equation contains the natural frequencies as well as the longitudinal load P which is contained in r_1 and r_2, (see equation 7). The natural frequencies can therefore be determined as a function of the longitudinal load. This was done by iteration. The results are presented in Figure 5 by the solid curves. Arbitrary values were chosen for the parameters. The only purpose of these preliminary numerical computations was to obtain a graphic picture of the relationship between load and natural frequency. The numerical values for these computations, such as the modulus of elasticity, static moment of inertia, etc. were rough estimates of the various spine materials.

The eigenfunctions for this set of boundary conditions are

$$V_n(x) = \sin r_{2n} x + \frac{r_{2n}^3 \cos r_{2n}\ell + \delta \sin r_{2n}\ell}{r_{1n}^3 \cosh r_{1n}\ell - \delta \sinh r_{1n}\ell} \sinh r_{1n} x \cdot \qquad (41)$$

These eigenfunctions depend also on the longitudinal load. The first eigenfunction at three different longitudinal loads is presented in Figure 6. The numerical values for the various parameters were chosen to represent a human subject. The length ℓ is 30.48 cm which

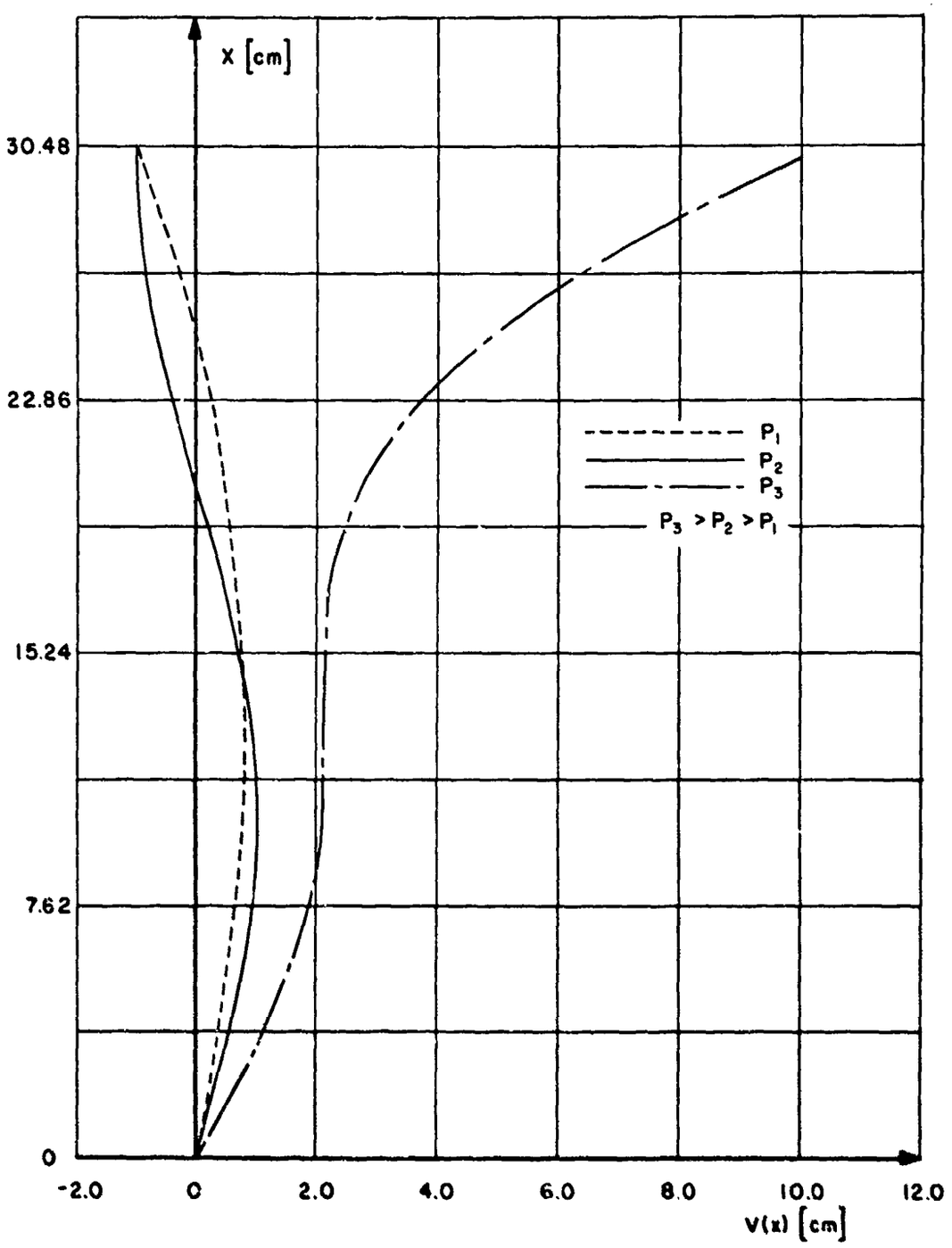

Figure 6. Eigenfunctions of Unrestrained Spine Model Under Various Longitudinal Loads.

represents the length of the average lumbar spine. The lowest of the longitudinal loads, P_1, is 27 lbs. or 12.27 kp, which is about the weight of the average human thorax. The load P_2 is three times that of P_1 and the load P_3 is ten times that of P_1. It is very obvious that these eigenfunctions depend very much on the longitudinal load. The curve for the load P_2 is in shape similar to the transverse displacement distribution along the lumbar spine of sitting human subjects under vertical vibration (Figure 2).

The bending moment along the spine in one of its eigenmodes is directly proportional to the second derivative of the eigenfunction. These derivatives are plotted in Figure 7 for the same three longitudinal loads. It is very obvious that these derivatives depend on the longitudinal load. The bending load is rather evenly distributed over the length of the lumbar spine at small longitudinal loads. Peaks of bending loads appear as the longitudinal load increases. The greatest peak occurs at the upper end and a smaller one at the lower section of the lumbar spine. The peaks increase with the longitudinal load and the lower peak moves farther down the spine.

Statistical curves have been published that show the incidence of vertebral injury along the lumbar and thoracic spine. These curves differ somewhat from one author to the other. Hirsch and Nachemson[4] arrive at a distribution along the lumbar spine that is fairly even. Moffatt and Howard[5] present one with an incidence of injury that is low at the lower end of the lumbar spine, increases slowly from there on up, and increases rapidly around the 11th and 12th thoracic vertebra. Another curve published by Higgins et al.[6] is similar to that of Moffatt except for no injuries around the 4th lumbar vertebra and some injury of the coccyx.

It seems that the differences of these curves may be due to differences in the magnitude of the longitudinal loads.

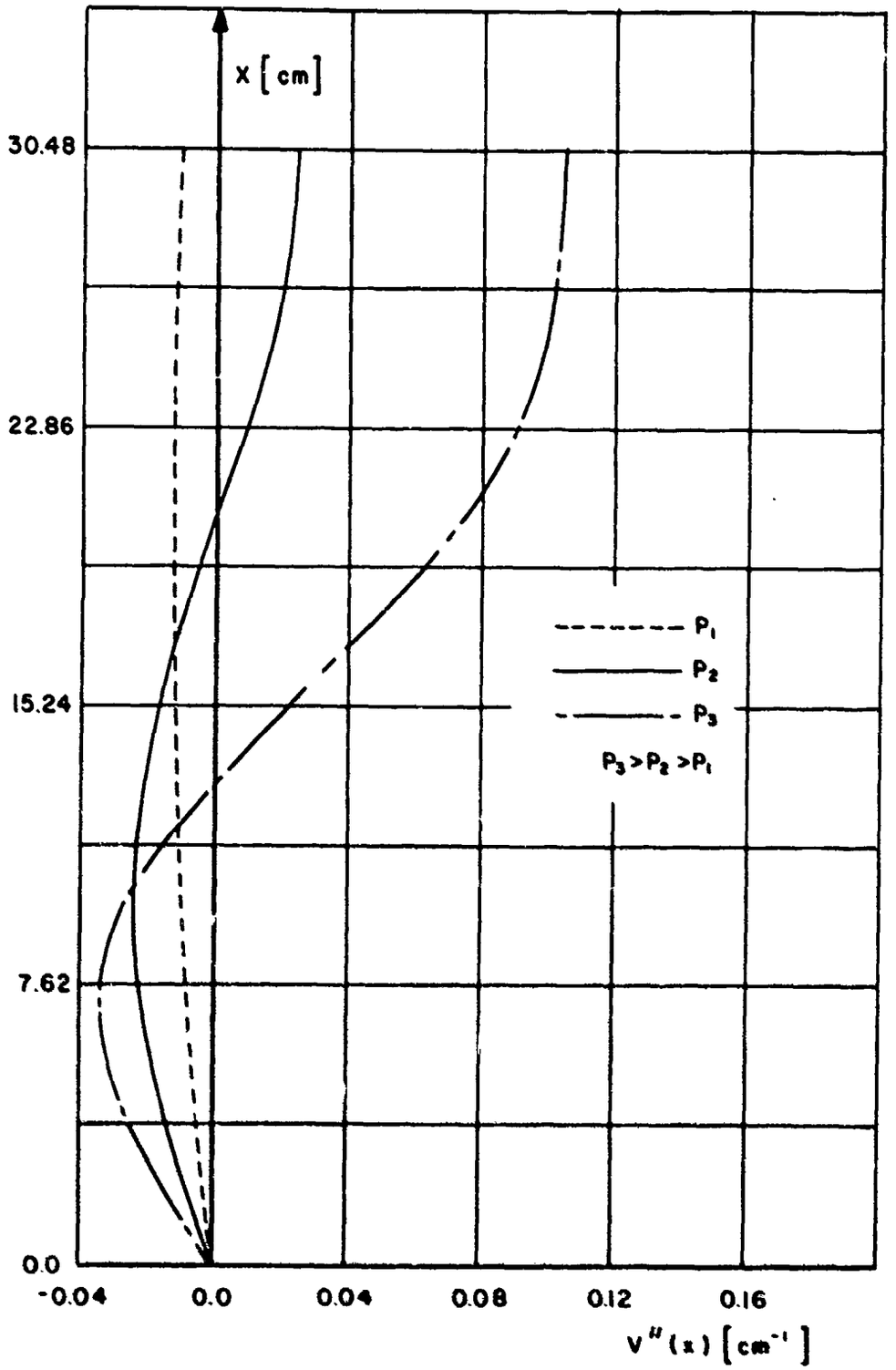

Figure 7. Second Derivative of Eigenfunctions of Unrestrained Spine Model Under Various Longitudinal Loads.

After comparison with the second derivative of the eigenfunction, one would expect the incidence curve of Hirsch and Nachemson to be obtained from cases of relatively small longitudinal loading. The second derivative of the eigenfunction crosses the zero line for two longitudinal loads. This seems to reflect the zero incidence in Higgins' curve around the 4th lumbar vertebra.

B. Curved Rod

In the previous discussion, we did not consider the right hand side of equation (1). The nonhomogeneous equation cannot be solved exactly by making a product assumption because it is not self adjoint. An approximate solution with such an assumption can be obtained. In this case, the Galerkin method will be applied.

The equation of motion is rearranged to assume the form

$$EI \frac{\partial^4 v}{\partial x^4} + P(t) \frac{\partial^2 v}{\partial x^2} + \mu \frac{\partial^2 v}{\partial t^2} + P(t) \frac{d^2 v_0}{dx^2} = L(v) = 0. \quad (42)$$

A product assumption of the following nature is made

$$\bar{v}(x,t) = \sum_{n=1}^{N} V_n(x)\, T_n(t) \quad (43)$$

where the $V_n(x)$ are the previously determined eigenfunctions. This is substituted into equation (42) which results in

$$L(\bar{v}) = \epsilon(x,t). \quad (44)$$

$\epsilon(x,t)$ is zero if such an assumption can satisfy equation (42) exactly, and it is different from zero if it cannot do that. In this case the error of an approximate solution with this assumption is minimized by imposing the conditions

$$\int_0^l L(\bar{v})\, V_n(x)\, dx = 0 \quad . \qquad n = 1, \ldots . N \tag{45}$$

This requires the error $\epsilon(x, t)$ along the length of the rod weighted by the eigenfunctions and integrated over x to be zero. In other words, equation (45) requires orthogonality between the residual and the eigenfunctions.

The variable x is eliminated through integration and a system of coupled ordinary differential equations with t as the variable evolves. These equations would not be coupled if the eigenfunctions of the adjoint problem would have been used for weighting functions. The coupled equations are in matrix notation

$$\{\ddot{T}_n\} + \frac{1}{\mu}[a_{nj}]^{-1}(EI[b_{nj}] + P(t)[C_{nj}])\{T_n\} = -P(t)[a_{nj}]^{-1}\{A_n\} \tag{46}$$

$$a_{nj} = \int_0^l V_n V_j\, dx \; ; \; b_{nj} = \int_0^l V_n V_j^{(4)}\, dx$$

$$C_{nj} = \int_0^l V_n V_j''\, dx \; ; \; A_n = \int_0^l \frac{d^2 v_0}{dx^2} V_n\, dx \tag{47}$$

The solution of this equation consists of the solution for the homogeneous equation plus a particular solution of the nonhomogeneous equation. An assumption of the type

$$\{T_i\} = \{T_{io}\} e^{i\omega t} \tag{48}$$

for the homogeneous equations, and the usual manipulations, leads to a solution of the type

$$T_n = \sum_{k=1}^{N} q_k \mu_{nk} \sin(\omega_k t + \psi_k) . \tag{49}$$

The μ_{nk} are the amplitude ratios.

The right side of equation (46) is constant. Therefore, a constant can be determined as a particular solution. This solution is

$$\{B_i\} = - P(t) [H]^{-1} [a_{ij}]^{-1} \{A_i\} \tag{50}$$

$$[H] = \frac{1}{\mu} [a_{ij}]^{-1} (EI[b_{ij}] + P(t) [c_{ij}]) \tag{51}$$

The complete solution is then

$$\bar{v}(x,t) = \sum_{n=1}^{\infty} V_n \sum_{k=1}^{N} (q_k \mu_{nk} \sin(\omega_k t + \psi_k) + B_n) . \tag{52}$$

This can be rearranged and expanded to assume the following form:

$$\begin{aligned} \bar{v}(x,t) = {} & q_1 [V_1\mu_{11} + V_2\mu_{21} + .. V_n\mu_{n1}] \sin(\omega_1 t + \psi_1) --- \\ & + q_n [V_1\mu_{1n} + V_2\mu_{2n} + .. V_n\mu_{nn}] \sin(\omega_n t + \psi_n) \\ & + \sum_{n=1}^{\infty} V_n B_n . \end{aligned} \tag{53}$$

The eigenfunctions of the curved rod under the specified boundary conditions can be expressed as series of the eigenfunctions of the straight rod weighted by the amplitude ratios as obtained during the solution for the time distribution.

The q_n have to be determined using the initial conditions. Various methods can be applied such as subdomain, Galerkin, or a collocation technique. In any case, the q_n will finally be dependent on the V_n, that

is the eigenfunctions, and on the B_n which are determined by the initial curvature. Therefore the amplitudes of the free motions are affected by both the initial curvature and the longitudinal load which is also part of the B_n's and the eigenfunctions. The initial curvature of the spine changes between different attitudes of a subject. The difference in response between attitudes can be accounted for through the initial curvature.

C. Dynamic Instability

The solution for the spatial and time distribution, equation (49), applies only if P(t) is a constant. The differential equation for the time distribution, equation (46), will have to be solved by procedures such as Hill's method. Of particular interest are areas of possible dynamic instability. These have not been determined for this particular case. However, these areas are usually around the lines of the natural frequencies in Figure 5 and also around curves of twice the natural frequency, fractions of it, and at frequencies that are the sums and differences of the natural frequencies. Some of these conditions of parametric instability are indicated by the broken lines in Figure 5.

CONCLUSIONS

It was the purpose of this discussion to investigate the possibilities of accounting quantitatively for the effect of longitudinal loads on the natural frequencies of transverse motions of the lumbar spine, as well as for the effects of longitudinal loading and initial curvature on the magnitude and distribution of bending along the lumbar spine.

Longitudinal loads, initial curvature and boundary conditions imposed on the lumbar spine seem to have significant effects on the magnitude and distribution of bending in a dynamic environment. The type of bending distribution curves that have been obtained seem to agree with statistical curves of injury incidence along the lumbar spine. The transverse displacement distribution along the lumbar spine under

longitudinal loads agrees with experimental data. A more detailed numerical adjustment of the model to experimental data will be attempted. In particular, major subsystems that are coupled to the spine will have to be considered for this purpose. Because subsystems have an effect on the boundary conditions and thus on the response of the spine, it seems they have to be included because no experimental data are available that exclude coupling effects.

The natural frequency of transverse spine motions under longitudinal loads is load-dependent. The natural frequency decreases in general with increasing compressive loading and increases with increasing tensile loading. The type of natural frequency - longitudinal load relationship depends to a great degree on the boundary conditions.

Parametric transverse resonances and dynamic instabilities can be expected under a periodic longitudinal load.

ACKNOWLEDGEMENTS

This research was jointly sponsored by the 6570th Aerospace Medical Research Laboratories under Air Force Contract F33615-69-C-1681 and the University of Dayton Research Institute (UDRI).

The authors gratefully acknowledge the assistance provided by personnel of the 6570th Aerospace Medical Research Laboratory, Vibration and Impact Branch, and the staff of the University of Dayton Research Institute. The authors are indebted to Dr. Jack Crouch (UDRI) for many suggestions and discussions.

REFERENCES

1. Vulcan, A. P., A. I. King and G. S. Nakamura, "Effects of Bending on the Vertebral Column During + G_z Acceleration," Aerospace Med., 41(3):294-300 (1970).

2. Krause, H., "Das schwingungsmechanische Verhalten der Wirbelsaeule," Int. Z. angew. Physiol. einschl. Arbphysiol, Vol. 20:125-155, (1962).

3. Bolotin, V. V., The Dynamic Stability of Elastic Systems, Holden-Day, Inc., San Francisco, (1964).

4. Hirsch, C. and A. Nachemson, "Clinical Observations on the Spine in Ejected Pilots," Acta Orth. Scand., 31, Fas. 2:135-145 (1961).

5. Moffat, C. A. and R. H. Howard, The Investigation of Vertebral Injury Sustained During Aircrew Ejection, Technology, Inc., San Antonio, Texas, Quarterly Progress Report No. 2, NASA Contract NAS2-5062.

6. Higgins, L. S., S. A. Enfield and R. J. Marshall, Studies on Vertebral Injuries Sustained During Aircrew Ejection, Final Report to Office of Naval Research, Contract No. NONR-4675 (00), Technology, Inc., San Antonio, Texas, (1965).